Reactive Compatibilization of SAN/EPR Blends. 2. Effect of Type and Content of Reactive Groups Randomly Attached to SAN

Christophe Pagnoulle and Robert Jérôme*

Center for Education and Research on Macromolecules (CERM), University of Liège, Sart-Tilman, B6, 4000 Liège, Belgium

Received May 15, 2000; Revised Manuscript Received October 10, 2000

ABSTRACT: Kinetics of the poly(styrene-*co*-acrylonitrile)/poly(ethylene-*co*-propylene) (SAN/EPR) interfacial reaction has been varied by changing both the average number of reactive groups per SAN chain and the content of reactive SAN in the SAN phase, while keeping constant the overall SAN/EPR composition, i.e., 75/25 w/w. For this purpose, reactive SAN chains containing 0.004, 0.028, 0.049, and 0.078 mol/wt % of either primary amine or carbamate (an amine precursor) have been synthesized, and the content of reactive SAN in the SAN phase has been changed from 2.5 to 73.33 wt %. It appears that the number and type of reactive groups attached onto SAN affect not only the extent of the compatibilization reaction but also the compatibilization capability of the in situ formed graft copolymer in a strong dependence on molecular weight and molecular architecture.

1. Introduction

The efficiency of reactive compatibilization of immiscible polymers pairs has already been studied in relation to the content of reactive groups of at least one polymer. De Roover et al.[1] have studied the effect of the content of maleic anhydride (MA) grafted onto polypropylene (PP-*g*-MA) on the average size of the PP phases dispersed in nylon 6. This size decreases rapidly with increasing content of grafted anhydride. However, beyond a critical content, the size levels off. Since maleic anhydride reacts almost quantitatively with the amine end groups of nylon 6, a direct relationship between size of the dispersed PP phase and extent of the grafting reaction has been proposed.

A Monsanto patent by Lavengood[2] has reported on the influence of the MA content of SAN on the notched Izod impact strength of acrylonitrile−butadiene−styrene terpolymer/polyamide 6 (ABS/PA 6) blends. When 6 wt % reactive SAN is used as compatibilizer, the impact strength is the highest in the case of SAN containing ca. 1 mol % MA. At higher MA contents, the PA6-*g*-SAN copolymer formed at the interface becomes rich enough in PA6 for leaving the interface in favor of the PA6 phase.

Baker et al.[3] have studied the compatibilization capability of glycidyl methacrylate grafted polypropylene (PP-*g*-GMA) copolymers of different glycidyl methacrylate (GMA) contents in PP/poly(acrylonitrile-*co*-butadiene-*co*-acrylic acid) (NBR) blends. Although the impact energy depends on the total amount of the GMA groups in the blend, it appears that this energy decreases when the average number of GMA groups per PP-*g*-GMA chain is increased at constant total GMA content. This observation has been discussed on the basis of both number and effectiveness of the interfacial entanglements in relation to the molecular structure of the PP-*g*-MA compatibilizer.

Duvall et al.[4] have compared the compatibilization efficiency of PP-*g*-MA of high and low anhydride content in PP/PA6 blends. Higher fracture strain was observed for the compatibilizer with the low anhydride content.

* To whom correspondence should be addressed.

It thus appears from these studies that there is an optimum degree of functionalization, beyond which the efficiency of the reactive compatibilizer decreases.

This study will devote special attention to the dependence of morphology and impact strength of SAN/EPR reactive blends on both the type and number of reactive groups attached onto SAN. For this purpose, neat SAN will be added with SAN chains containing various amounts of either primary amine or carbamate (precursor of NH_2), i.e., type a, 0.004 (0.3); type b, 0.028 (2); type c, 0.049 (4); and type d, 0.078 (8) mol of NH_2 or carbamate/wt % (mol %). The composition of the EPR phase is kept constant (i.e., 50 wt % EPDM and EP-*g*-MA). The SAN/EPR wt composition will be systematically 75/25, the mixing time 7 min, and the blending temperature 200 °C. These experimental conditions are well-suited to study the influence of the compatibilization reaction kinetics, since the copolymer formation is a second-order reaction:[5]

$$v = k_x[X]_0[MA]_0 \quad (1)$$

v and k_x are the initial rate and the rate constant, respectively, for the NH_2(carbamate)−maleic anhydride interfacial reaction, and $[X]_0$ and $[MA]_0$ are the initial molar concentration of NH_2 (carbamate) and maleic anhydride (mol/vol), respectively, in the blend. Equation 1 is only valid to homogeneous reaction, which is not the case of the reactive system under consideration. The reactive SAN/EPR compatibilization basically occurs at the interface, so that the concentration of reactive species has to be calculated in this area, which actually changes as reaction proceeds.[6] Under these conditions, and as a crude approximation, $[X]_0$ and $[MA]_0$ are proportional to the interfacial area which will be considered constant for all the SAN/EPR blends, i.e., in the early stage of mixing (v being the initial reaction rate constant in eq 1), and for the same rubber content (25 wt %). $[MA]_0$ is also a constant in all the experiments. $[X]_0$ is proportional to the content of reactive of SAN−X in the blends and to the content of reactive groups (X = NH_2 or carbamate) per chain (RGC). Therefore, eq 1 can be rearranged.

10.1021/ma000822g CCC: $20.00
Published on Web 01/12/2001

$$v = k_x' \, \mathrm{RGC}[\mathrm{SAN{-}X}]_0 \qquad (2)$$

From eq 2, it appears that the impact properties and phase morphology of the reactive polyblends have to be discussed on the basis of the three main reaction parameters, i.e., the intrinsic reactivity of the X functional groups (taken into account by k_x'), the content of X groups per SAN chain (RGC), and the initial amount of SAN−X calculated per volume unit of the polyblend ($[\mathrm{SAN{-}X}]_0$).

2. Experimental Section

2.1. Materials. SAN used in this work was the RONFALIN 2770 from DSM containing 26.5 wt % (40 mol %) acrylonitrile. The maleic anhydride grafted poly(ethylene-*co*-propylene) (EP-*g*-MA), EXXELOR VA 1801 from Exxon, contained 0.6 wt % succinic/maleic anhydride groups (or 6×10^{-3} mol/wt %). The nonreactive rubber was the EPDM, KELTAN 4778, from DSM. Terpolymerization of styrene, acrylonitrile, and a carbamate-containing comonomer, {1-methyl-1-[3-{1-methylethenyl)-phenyl]ethyl}carbamic acid 1, 1-dimethylethyl ester or TMIT-BC, was initiated by AIBN (2 mol %) in toluene at 60 °C for 24 h. It was recovered by precipitation in methanol. Concentration of these functional groups has been varied in this work in the range of 0.004−0.078 mol/wt % (Table 1).

The partial overlapping of the ^{1}H NMR peak assigned to the *tert*-butyl group of the carbamate containing comonomer (at 1.40 ppm) with the signal for the aliphatic CH makes impossible the quantitative analysis of this monomer composition. The resonance of the single NH proton at 4.9 ppm is however too weak and too broad for the composition analysis to be ascertained. Conversely, the carbamate-containing comonomer (TMITBC) in the terpolymer is easily identified by a strong IR absorption of the carbamate at 1717 cm^{-1}, which persists upon purification of the copolymer by solvent extraction and precipitation. The copolymer was redissolved in acetone and reprecipitated from MeOH, which is a good solvent for the carbamate-containing monomer. This purification cycle was repeated at least three times, and no residual vinyl protons were found by NMR. Terpolymer composition was determined by FTIR on the basis of a calibration curve. For this purpose, blends of SAN (Ronfalin 2770 from DSM, 26.5 wt % acrylonitrile) and TMITBC of various molar compositions were dissolved in chloroform and solvent cast on NaCl disk for FTIR anlysis. The ratio of the carbamate absorption (at 1717 cm^{-1}) over the nitrile absorption (2236 cm^{-1}), i.e., $A_{carb}/A_{nitrile}$, was plotted vs the TMITBC/AN comonomer molar ratio ($A_{carb}/A_{nitrile} = 17$ [TMITBC]/[AN]). The absorption of the aromatic C=C (1601 cm^{-1}) over the carbamate absorption (at 1717 cm^{-1}), i.e., A_{aro}/A_{carb}, was also plotted vs the styrene/TMITBC comonomer molar ratio ($A_{aro}/A_{carb} = 0.147 + 0.036$ [styrene]/[TMITBC]). Table 1 shows that the mole fractions of the electron donor monomers (styrene + TMITBC) and the electron acceptor monomer (AN) fit the azeotropic ratio, i.e., 60/40 (styrene + TMITB)/AN in mol %. Since the azeotropic styrene/AN comonomer feed ratio has been systematically used, this feature suggests that TMITBC has been polymerized at the expense of styrene, without changing the original distribution of the comonomers in the chain. Since TMITBC is in large defect with respect to styrene, it is thought to be randomly distributed along the terpolymer chain.

The carbamate pendant groups of functional SAN were derivatized into amines either in solution prior to blending[7] or in situ during the blending process.[8] These two approaches were investigated. The amine released by the acidic hydrolysis of SAN−carb was analyzed not only by acid−base titration but also by size exclusion chromatography with an UV detector which required SAN−NH_2 to be tagged previously by dinitrofluorobenzene (DNFB).[9]

The amine content was estimated by non aqueous acid−base titration in a toluene−methanol (9:1) mixture (potentiometric titration) using a standard solution of $HClO_4$. An error of 5% was found with respect to the carbamate content of the terpolymer (determined by FTIR).

Table 1. Molecular Characteristics of Reactive SAN

SAN−X[a] sample	RGC (mmol X/wt %)	S/AN/X (mol %)	M_n[b] (10^3 g/mol)	M_w/M_n[b]	SAN/SAN−X miscibility
a	4	59/40/0.3	114	1.75	yes
b	28	57/40/2	122	1.90	yes
c	49	55/40/4	110	1.80	yes
d	78	52/40/8	109	1.85	no

[a] All these samples are available with X = NH_2 and carbamate. [b] SEC calibrated with polystyrene standards.

The NH_2 groups of the copolymer were converted into substituted dinitroaniline by reaction with DNFB under the usual conditions. The tagged copolymer was analyzed in THF with a size exclusion chromatograph equipped with a differential refractive index detector (sensitive to the polymer concentration) and a UV detector operating at 350 and 405 nm, respectively (sensitive to the DNFB concentration). It was ascertained that the absorption at 350 and 405 nm by the unlabeled terpolymer was negligible. A very close agreement for the elution times measured by the UV detector (at two wavelengths) and the RI detector was found (a systematic difference of 0.2 min resulted from the technical characteristics of the SEC apparatus), confirming that the amine functionality (amine tagged by DNFB) is directly associated with the polymer. The shape of the elution peak is basically independent of the detector, which indicates that the DNFB (and thus primary amine) distribution in the copolymer is essentially independent of molecular weight. Thus, DNFB has reacted selectively with the primary amine groups, and copolymerization of TMITBC with styrene and acrylonitrile is effective.

2.2. SAN/SAN−X Phase Behavior. SAN was mixed with 25 wt % reactive SAN in chloroform, and the clear solution (5 wt %) was cast on a glass plate. $CHCl_3$ was let to evaporate under a $CHCl_3$ saturated atmosphere at 25 °C (for at least 24 h), so as to maintain the system as close to equilibrium as possible. Films were finally dried in a vacuum oven (24 h at 80 °C). Glass transition temperatures (T_g's) of SAN and reactive SAN−X ($T_g \sim 110$ °C) were too close to each other for any phase separation to be ascertained by T_g measurements. Therefore, miscibility was analyzed by visual and microscopic observation of the solvent-cast films. When SAN−X contained 0.078 mol/wt % functional groups, hazy films were formed, indicating phase separation whatever the functional group, NH_2 or carbamate. Optical microscopy showed dark domains of modified SAN-rich phases. The phase demixing persisted not only after annealing at 150 °C (thus above T_g of each blended polymer) for 24 h but also up to the highest temperature investigated (i.e., 300 °C), thus indicating the absence of upper critical solution. When the RGC of SAN−X is smaller (0.004, 0.028, or 0.049 mol/wt % either carbamate or primary amine), all the blends were transparent up to at least 300 °C. This observation by the naked eye was confirmed by optical microscopy.

2.3. Mixing Conditions. Samples (20 g) were melt blended with a laboratory two-roll mill at 200 °C. A master batch of 50 wt % EPDM and EP-*g*-MA was previously melt blended for 7 min under moderate shearing (rolls speed = 15 and 25 rpm) and stabilized by 0.5 wt % IRGANOX 1010 from Ciba Ceigy. After mixing, the rubbery blend was cooled to room temperature and cut into small pieces (2 × 5 mm). An appropriate amount of reactive SAN−X was then melt blended with neat SAN at 200 °C for ca. 2 min, followed by the addition of the required amount of the (EPDM/EP-*g*-MA) premixture. One minute later, the shear rate was regularly increased (rolls speed of 0.5 and 25 rpm). The mixing conditions were maintained for an additional 6 min. This two-step mixing resulted from preliminary optimization, according to which the rubber dispersion was better when small rubber particles were used rather than preheated rubber.[10−12]

After mixing, the samples were rapidly compression molded into sheets (2 mm thick) at 200 °C for 5−7 min and then allowed to cool to room temperature.

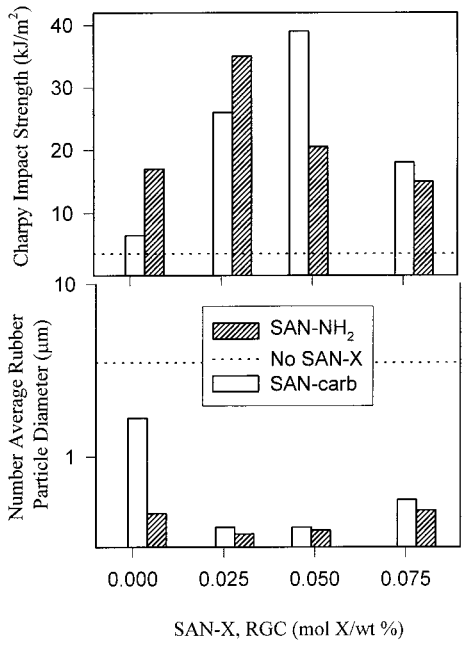

Figure 1. Dependence of both the impact strength and the number-average rubber particle diameter on the SAN reactive groups content (type a, 0.004; type b, 0.028; type c, 0.049; type d, 0.078 mol/wt % of either NH_2 or carbamate) for the 75/25 SAN/EPR blend modified by 33 wt % SAN−carb(NH_2) in the SAN phase and 50 wt % EP-*g*-MA in the EPR phase.

2.4. Interfacial Grafting Conversion. The extent of the interfacial grafting was quantified by a solvent extraction technique. Samples of pelletized blends (1.0 g) were extracted by refluxing acetone (selective solvent for SAN) in a Soxhlet apparatus up to constant weight, i.e., for at least 100 h. The insoluble material was recovered and dried up in a vacuum oven. The soluble fraction was concentrated and precipitated into methanol. Films of the insoluble material were compression molded at 200 °C for 1 min and quantitatively analyzed by FTIR in order to estimate the amount of SAN grafted to the rubber phase. The amount of rubber in the soluble fraction appeared to be negligible.[13,14]

2.5. Transmission Electron Microscopy. Observations were conducted with the transmission electron microscope Philips M100 at an accelerating voltage of 100 kV. Thin sections (90 nm) were prepared by ultramicrotomy (Ultracut E from Reichert-Jung) at −130 °C and stained by exposure to RuO_4 vapors for ca. 2 h. SAN was observed as darker phases as result of higher affinity for ruthenium tetroxide compared to EPR. Micrographs were analyzed by using the KS 100 (Kontron Imaging System) software. An average number of 300 particles (dispersed phases) were considered per sample. The cross-sectional surface area of these particles was converted to an equivalent diameter by eq 3:

$$d_{\text{equivalent}} = (4/\pi(\text{area}))^{0.5} \quad (3)$$

2.6. Mechanical Testing. Tensile and impact test specimens were machined from molded sheets and stored at room temperature for 2 days before analysis. Sheets were compression molded at 200 °C and 20 MPa for 5−7 min and quenched under a low pressure. Stress−strain curves were recorded at room temperature with an Instrom tester (model DY24) at 20 mm/min tensile speed, using specimens prepared according to the DIN 53488 standard. The notched Charpy impact strength was measured at room temperature with a Ceast fractoscope using ASTM D256B notched specimens (0.35 mm notch).

3. Results and Discussion

Figure 1 illustrates the basic effect that content of reactive groups in SAN−X and nature of X (amine or carbamate) have on the impact strength and the number-average diameter, D_n, of the rubber particles for 75/25 SAN/EPR polyblends. In the case of SAN−NH_2, the best improvement of the impact strength is observed at an intermediate NH_2 content, thus in the vicinity of 0.028 mol/wt %. When the RGC of SAN−NH_2 is increased from 0.004 to 0.028 mol/wt %, the impact strength is increased, as result of more probable interfacial grafting in qualitative agreement with eq 2. In parallel, the rubber dispersion becomes finer. However, the situation dramatically changes when the RGC of reactive SAN exceeds 0.028 mol/wt %. A sharp drop in the impact strength is then observed, whereas D_n remains almost unchanged.

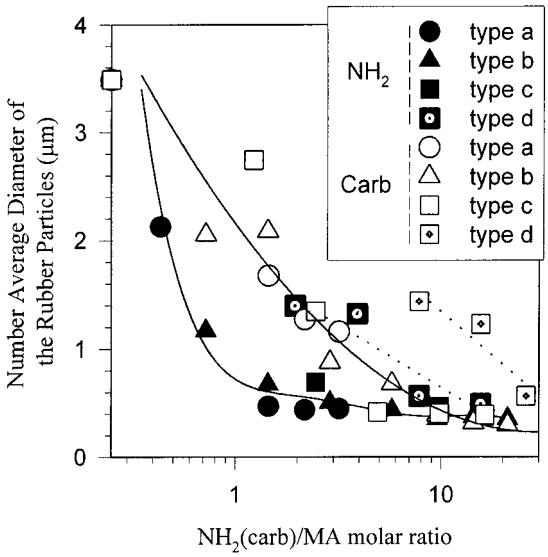

Figure 2. Dependence of the number-average rubber particle diameter on the carb(NH_2)/MA molar ratio for the 75/25 SAN/EPR polyblend modified by SAN−carb(NH_2) of various reactive groups contents (type a, 0.004; type b, 0.028; type c, 0.049; type d, 0.078 mol/wt % of either NH_2 or carbamate) in the SAN phase and 50 wt % EP-*g*-MA in the EPR phase.

The intrinsic reactivity of the SAN functional groups, k_x', is also of a prime importance. Indeed, the best improvement in impact strength is observed for a SAN−carb content of 0.049 mol/wt % (type c) compared to 0.028 mol/wt % (type b) in the case of SAN−NH_2. This observation is in line with the lower reactivity (toward maleic anhydride) of SAN−carb.[13,14]

At very high content of reactive groups, either NH_2 or carbamate (0.078 mol X/wt %, type d), demixing of neat SAN and reactive SAN occurs and is certainly detrimental to ductility and phase morphology (D_n).

These experimental observations show that an optimum in the properties depends on the way the grafting reaction is conducted and suggest that the impact strength depends on the phase morphology. This dependence is discussed below on the basis of the SAN reactive groups (NH_2 or carbamate) over maleic anhydride molar ratio.

3.1. Emulsification Curve. For a series of eight blends which differ in the type and number of reactive groups attached to reactive SAN, the number-average rubber particle diameter, D_n, has been plotted versus the [X]/[MA] (X stands for NH_2 or carbamate, and [X] has been determined by multiplying the RGC of SAN−X by its wt content in the blend) molar ratio in Figure 2. The rubber particle size actually depends on this ratio, although in a way that depends on the intrinsic reactivity of the SAN reactive groups.

Table 2. Experimental Data on the Phase Morphology and Impact Strength (IS) for the 75/25 SAN/EPR Polyblend[a]

		morphology				impact resistance			
type	X	k^b	$X/MA_{crit}{}^c$	SAN−X_{crit} (wt %)	$D_{eq}{}^d$ (μm)	IS[e] (kJ/m^2)	X/Ma_{crit}	SAN−X_{crit} (wt %)	Imp_{max} (kJ/m^2)
a		0.57	−	−	−	3	−	−	−
b	carb	0.57	∼7	25	0.38	3	∼20	73	39
c		0.57	∼7	14	0.38	3	∼20	40	43
d		−	−	−	−	1	∼20	16	18
a		1.88	∼2	46	0.41	10	−	−	−
b	NH_2	1.88	∼2	7	0.41	6	∼5	18	35
c		1.88	∼2	4	0.41	4	∼5	10	21
d		−	−	−	−	2	∼8	10	15

[a] The EPR phase contains 50 wt % EP-*g*-MA and the SAN phase different amounts of SAN−X of various reactive groups contents: 0.004 (type a), 0.028 (type b), 0.049 (type c), and 0.078 (type d) mol X/wt % (X being NH_2 or carbamate). [b] Values of k in eqs 5 and 6. [c] [X]/[MA] molar ratio at the equilibrium particle size (from eqs 5 and 6). [d] Equilibrium particle size approximated from eqs 5 and 6. [e] Initial slope (IS) of the dependence of the impact strength on the [X]/[MA] molar ratio.

These typical emulsification curves[15] confirm that the rubber particle diameter first decreases rapidly when the [X]/[MA] ratio is increased (regime 1), as result of the enhanced probability for the interfacial reaction (thus grafting) to occur (eq 1). Beyond a critical molar ratio, i.e., $[X]/[MA]_{crit}$, this decrease in D_n sharply changes for becoming very slow (regime 2). According to Tang and Huang,[16] these emulsification curves can be approximated by eq 4:

$$D = (D_0 - D_{eq})e^{-k([X]/[MA])} + D_{eq} \quad (4)$$

where D_0 and D_{eq} are the average size of the dispersed phase when the content of SAN reactive groups is zero and at saturation, respectively, and k is the rate constant for the change in diameter in relation to the [X]/[MA] molar ratio.

In the case of SAN−NH_2 and for amine contents between 0.004 and 0.049 mol/wt %, the major reduction of the rubber particle size (from ca. 3.5 in absence of reactive SAN down to 0.7 μm) occurs, when the molar ratio is increased from 0 to 1 (Figure 2). At constant total amount of SAN reactive groups in the blends, a higher RGC means that less reactive SAN chains are required to reach a comparable particle size (Table 2). The unique emulsification curve that fits the experimental D_n observed for SAN−NH_2 containing 0.004, 0.028, and 0.049 mol NH_2/wt % is expressed by eq 5:

$$D = (3.49 - 0.41)e^{-1.88([X]/[MA])} + 0.41 \quad (5)$$

This equation shows that the average diameter of the dispersed phase tends to a constant value of 0.41 μm.[16]

The emulsification curve is shifted toward higher NH_2/MA molar ratios, when the number of NH_2 per SAN chain exceeds 0.049 mol/wt % (type d); more likely, the SAN/SAN−NH_2 (type d, 0.078 mol NH_2/wt %) demixing is at the origin of this effect.

The emulsification curves are also shifted toward higher [X]/[MA] molar ratios, when SAN−carb is substituted for SAN−NH_2, consistent with the lower reactivity of carbamate toward maleic anhydride.[13,14] Within the limits of miscibility of SAN−carb with neat SAN (thus except for type d), the emulsification equation is as follows:

$$D = (3.49 - 0.38)e^{-0.57([X]/[MA])} + 0.38 \quad (6)$$

Although the equilibrium particle size, 0.38 μm, is quite similar to the value found in the case of SAN−NH_2 (0.41 μm), the k value is decreased by at least a factor of 3. Table 2 shows that the critical [X]/[MA] molar ratio, at which the equilibrium particle diameter is observed, is ca. 7 for SAN−carb compared to 2 for SAN−NH_2. It is clear that the phase morphology is largely controlled by the total amount of SAN reactive groups, in a strong dependence on their intrinsic reactivity toward maleic anhydride groups attached onto EP-*g*-MA. This behavior is strong evidence that the rubber dispersion is dictated by the interfacial grafting, such that the decrease in D_n with the content of SAN reactive groups is the signature of the beneficial effect of interfacial bonding. The difference in reactivity of the two types of reactive groups can be roughly expressed by the ratio of the k values (eqs 5 and 6), i.e., $k_{NH_2}/k_{carb} = 3.3$. So, compared to primary amines, 3.3 times more carbamate groups are required to provide comparable particle size. Consistently, a single master curve is obtained for both SAN−NH_2 and SAN−carb compatibilized blends, when the carbamate content is divided by 3.3 in the [carb]/[MA] molar ratio, at least within the range of SAN/SAN−X miscibility (Figure 3). This curve confirms the previous observation that the phase morphology strongly depends on the rate at which the phase morphology is developed compared to the compatibilization reaction in relation to the dispersion mechanism.[13,14] It must be recalled[13,14] that the reaction rate in polyblends modified by 20 wt % SAN−carb of

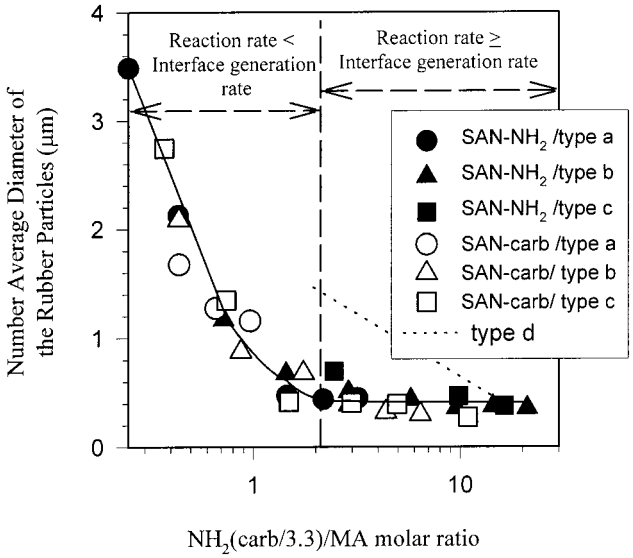

Figure 3. Dependence of the number-average rubber particle diameter on the reduced carb(NH_2)/MA molar ratio for the 75/25 SAN/EPR polyblend modified by SAN−carb(NH_2) of various reactive groups contents (type a, 0.004; type b, 0.028; type c, 0.049; type d, 0.078 mol/wt % of either NH_2 or carbamate) in the SAN phase and 50 wt % EP-*g*-MA in the EPR phase.

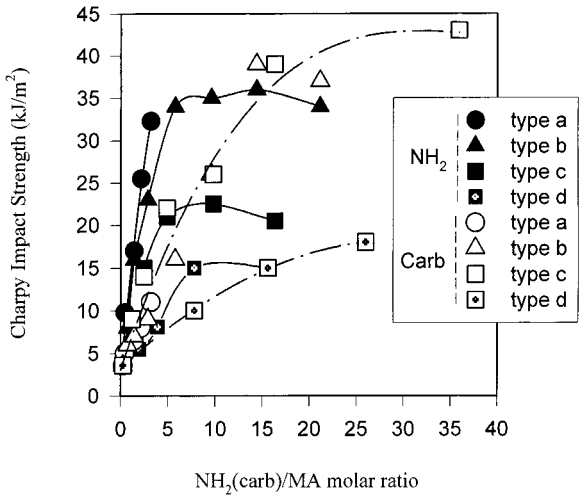

Figure 4. Dependence of the notched Charpy impact strength on the carb(NH_2)/MA molar ratio for the 75/25 SAN/EPR polyblend modified by SAN−carb(NH_2) of various reactive groups contents (type a, 0.004; type b, 0.028; type c, 0.049; type d, 0.078 mol/wt % of either NH_2 or carbamate) in the SAN phase and 50 wt % EP-*g*-MA in the EPR phase.

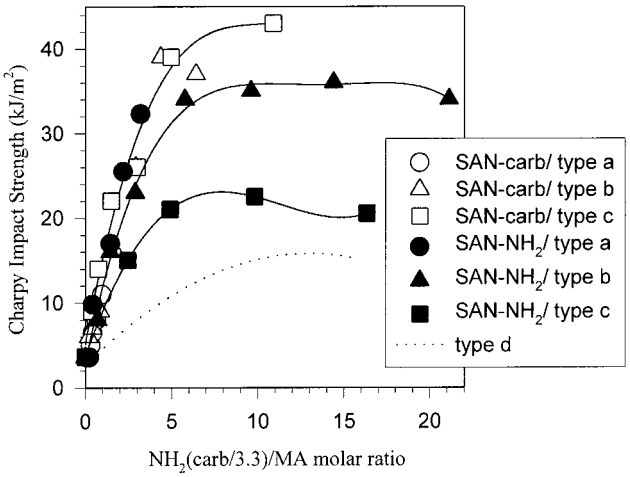

Figure 5. Dependence of the notched Charpy impact strength on the reduced carb(NH_2)/MA molar ratio for the 75/25 SAN/EPR polyblend modified by SAN−carb(NH_2) of various reactive groups contents (type a, 0.004; type b, 0.028; type c, 0.049; type d, 0.078 mol/wt % of either NH_2 or carbamate) in the SAN phase and 50 wt % EP-*g*-MA in the EPR phase.

type b (actual [X]/[MA] molar ratio = 5.70 or reduced ratio = 1.75; regime 1 of the emulsification curve in Figure 3) is controlled by the carbamate thermolysis into primary amine. This conclusion suggests that the reaction rate is slower than the rate at which the interface is formed. In contrast, when SAN−NH_2 is substituted for SAN−carb (actual or reduced [X]/[MA] molar ratio = 5.70; regime 2 of the emulsification curve), the interfacial reaction rate is much faster and the interface formation would be the rate-determining step. So, the SAN-*g*-EP copolymer would be rapidly formed (during the melting/softening of the constitutive polymers) in a sufficient amount to stabilize the interface as soon as it is formed. It may be inferred from Figure 3 that the equilibrium particle size is reached when the reaction rate equals the rate of interface generation, i.e., at a reduced [X]/[MA] molar ratio of ca. 2.

At a constant reduced [X]/[MA] molar ratio, the extent of the emulsification process is the same whatever the type of reactive groups (amine or carbamate) and their number per reactive SAN chains. Thus, the rubber dispersion is dictated by the interfacial grafting, such that 3.3 times more carbamate groups than primary amines are required to form rubber particles of the same size (eqs 5 and 6). From comparison of eq 1 and eqs 5 and 6, respectively, it might be inferred that the apparent rate constant for the maleic anhydride−amine reaction should be 3.3 times higher than that one for the carbamate−maleic anhydride reaction, i.e., $k'_{NH_2} = 0.0277\ min^{-1}$ since the carbamate grafting is controlled by the carbamate thermolysis into primary amine, whose the rate constant rate is $0.0084\ min^{-1}$.[13,14]

It is worth noting that the interface saturation by graft copolymer is not required for equilibrium particle size to be reached.[20,21] Inoue et al. found that ca. 20% surface coverage by block copolymer is enough to stabilize phase morphology against coalescence, which basically dictates the particle size.[22] Meanwhile, beyond a critical reduced [X]/[MA] molar ratio or reaction conversion, the rubber particle size levels off, while the interface covering with graft copolymer is still in progress.

3.2. Impact Resistance. Figure 4 shows the dependence of the Charpy impact strength on the SAN reactive group (i.e., NH_2 or carbamate) over maleic anhydride molar ratio. Nonreactive SAN/(EPDM/EP-*g*-MA) blend is brittle and has an impact strength of ca. 3.6 kJ/m² at room temperature. Upon addition of reactive SAN, the impact strength is rapidly improved, in a way that however depends on both the number and the type of reactive groups attached onto SAN.

The dependence of the impact strength on the carbamate over maleic anhydride molar ratio is essentially the same for SAN−carb containing 0.004, 0.028, and 0.049 mol carbamate/wt % (Figure 4). The impact strength first increases rapidly with the [carb]/[MA] ratio and then levels off beyond an actual molar ratio of ca. 20. However, the situation changes dramatically, when the SAN carbamate content exceeds 0.049 mol/wt %. A sharp drop in impact strength is observed, more likely as result of (SAN/SAN−carb) demixing. Thus, within the limits of miscibility, the mechanical performances of polyblends modified by SAN−carb are basically independent of the SAN carbamate content and essentially controlled by the total amount of these functional groups.

In the case of SAN−NH_2, the impact strength initially increases more rapidly compared to the SAN−carb counterpart, consistent with a higher reactivity (see Table 2). Figure 4 shows that the impact strength actually depends on the [NH_2]/[MA] molar ratio, in relation to the SAN amine group content. The compatibilization capability of the reactive SAN decreases as the NH_2 RGC is increased, at a constant [NH_2]/[MA] molar ratio. This suggests that more SAN chains of low amine content impart higher impact energy to the SAN/EPR blends than less SAN chains of high RGC, the total amount of amine being the same. This behavior is thus in sharp contrast to the independence of the impact resistance of the RGC of SAN−carb chains.

The difference in reactivity between amine and carbamate has also been taken into account in dividing the carbamate content by 3.3 and replotting the Charpy impact strength vs the reduced [X]/[MA] molar ratio in Figure 5. The experimental curves for SAN−carb containing 0.004, 0.028, and 0.049 mol carbamate/wt % are close to superposition. In the case of SAN−NH_2 of low

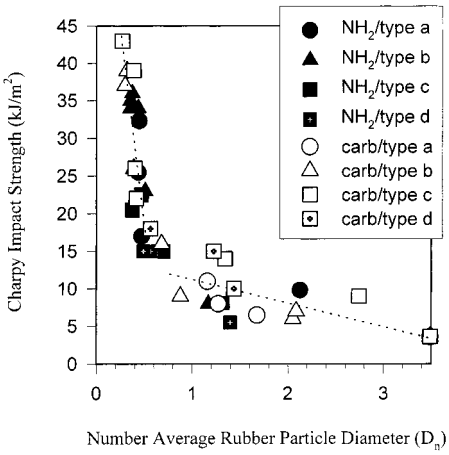

Figure 6. Dependence of the notched Charpy impact strength on the number-average diameter of the dispersed rubber particle for the 75/25 SAN/EPR polyblend modified by SAN−carb(NH_2) of various reactive groups contents (type a, 0.004; type b, 0.028; type c, 0.049; type d, 0.078 mol/wt % of either NH_2 or carbamate) in the SAN phase and 50 wt % EP-*g*-MA in the EPR phase.

RGC (type a, 0.004 mol NH_2/wt %), the curve is close to that one for SAN−carb, whereas this experimental dependence is regularly shifted toward lower impact strengths, as the RGC exceeds 0.004 mol NH_2/wt %. Therefore, depending on the reactive groups, the extent of SAN functionalization (RGC) affects in different ways the impact resistance, which was not the case of particle size (Figure 3).

3.3. Phase Morphology−Impact Resistance Relationship. It is usually accepted that the mechanical properties of polyblends are controlled by their phase morphology and, particularly, that the toughness of a brittle matrix is most improved when an optimum rubber particle size is reached. This toughening effect is consistent with the propagation of crazes which is more efficiently stopped when particle size is comparable to the craze thickness, for instance 0.75 ± 0.15 μm in poly(styrene-*co*-acrylonitrile).[17−19] Comparison of Figures 3 and 5 suggests that the refinement of the rubber dispersion is favorable to the impact resistance. Nevertheless, other experimental parameters have also to be considered. Indeed, whatever the reactive groups attached to SAN, the impact strength levels off at a higher critical reduced [X]/[MA] molar ratio (ca. 5) compared to the equilibrium particle (ca. 2). This observation suggests that the interfacial grafting has a more decisive effect on the mechanical properties than on the control of the rubber dispersion. In other words, the interface does not need to be saturated by graft copolymer in order to prevent the coalescence of the dispersed rubber droplets,[20,21] in contrast to the impact strength that needs a more extensive interfacial modification. As a second piece of formation, the plateau value of impact strength changes with the number of amine groups attached to SAN, whereas the final particle size is independent of the RGC of SAN−NH_2.

Figure 6 clearly shows that the relationship between notched Charpy impact strength and the number-average diameter of the rubber particles is complex, since there is a critical rubber particle diameter (0.5−0.75 μm), at which this dependence drastically changes. This critical size is close to the optimum particle diameter proposed by Wu for a SAN matrix.[19] In addition to the rubber particle size, the interfacial adhesion between rubber particles and brittle matrix has been shown to play a major role in the control of the impact absorbing properties.[23]

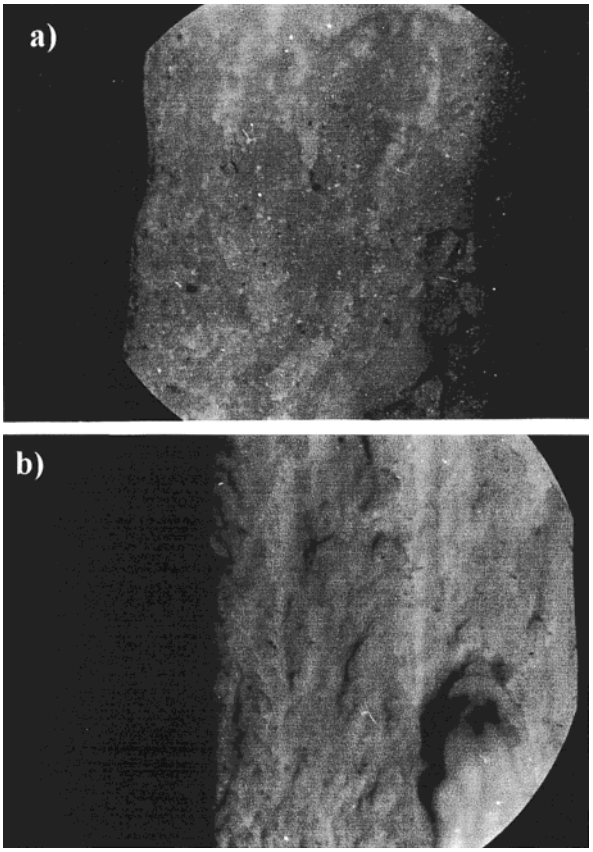

Figure 7. Optical microscopy of impact fracture surfaces for (a) a brittle sample and (b) a ductile sample.

3.4. Interfacial Adhesion. A strong interfacial adhesion is required to impart toughness to brittle matrix merely because craze termination cannot operate when rubber particles are detached from the matrix.[24−26] To analyze the effect of the in situ formed SAN-*g*-EP copolymer on the interfacial adhesion, the fracture surface caused by the Charpy impact test has been examined by scanning electron microscopy. Three main fracture mechanisms have been identified.

The failure mechanism changes from brittle fracture (<30 kJ/m^2) to ductile fracture (>30 kJ/m^2) with significant stress whitening, when sufficient amount of reactive SAN is added (Figure 7). Fracture of low impact specimens clearly shows that the rubber particles are pulled out of the matrix (Figure 8), which indicates a weak interfacial adhesion and prevents the energy from being dissipated efficiently into the rubber phase. The situation changes dramatically when high-impact polyblends are concerned. Near the notch, SEM cannot discriminate the two constitutive components, i.e., SAN and EPR, the fracture surface is smooth, and no evidence for the pullout of rubber particles is observed (Figure 9a). Far from the notch (Figure 9b), the rubber particles are extensively drawn. The tapered ends of thin drawn-out rubber tongues is in favor of the rupture rather than the debonding of the rubber component, thus of a strong rubber/SAN interfacial adhesion. Finally, fracture mechanism is different in the case of SAN−X of high RGC. Indeed, when content of SAN reactive groups exceeds 0.049 and 0.028 mol X/wt % in the case of SAN−carb and SAN−NH_2, respectively,

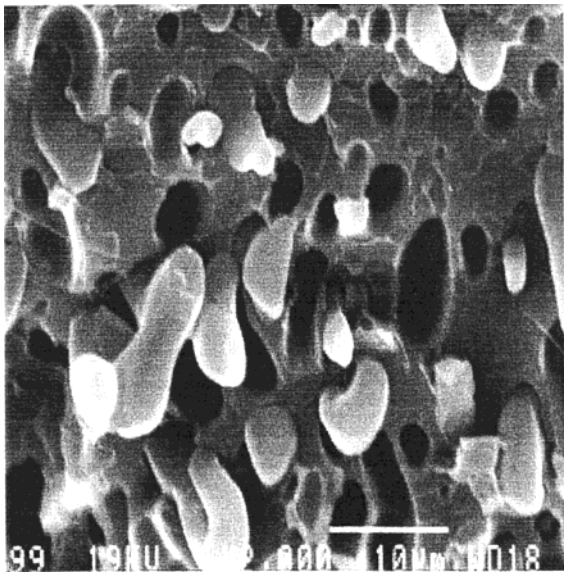

Figure 8. SEM of the impact fracture surface of the SAN/(EPDM/EP-*g*-MA 1/1) 75/25 blend.

holes are clearly observed far from the notch (Figure 10a), indicating particles debonding, whereas higher magnification (Figure 10b) shows several particles covered by a thin SAN layer. This observation indicates a loss of interfacial adhesion when the RGC is too high. Although SAN/SAN−X (type d) demixing might be at the origin of this effect,[27] the explanation does not hold in the case of SAN−NH_2 of type c, which is miscible with neat SAN. It thus appears that an excess of amine groups per chain is detrimental to the anchoring of the grafted chains to the SAN matrix, resulting in a sharp decrease of toughness (see Figure 1). It might accordingly be speculated that, although the interfacial adhesion must increase with the number of bridges at the interface, the effectiveness of the entanglements of the grafted SAN chains and the SAN matrix depends on both the degree and type of SAN functionalization in close relationship to molecular weight[28−30] and molecular architecture[31] of the SAN-*g*-EP copolymer.

3.5. Interfacial Grafting of SAN−X. The amount and molecular architecture of the grafted copolymer formed at the interface are expected to depend on the kinetics and completeness of the interfacial reaction in relation to the molecular characteristics of SAN−X. In this respect, a solvent extraction technique has been developed in order to estimate the amount of reactive SAN bound to the rubber phase. This information has however not been searched for in the case of highly functional SAN−X (type d, 0.078 mol X/wt %), which immiscible with SAN. Figure 11 shows how the weight fraction of SAN grafted to the rubber phase (with respect to the SAN phase), *W*, depends on the reduced [X]/[MA] molar ratio (in which the carbamate content is divided by 3.3).

It is clear that the experimental conversions for the SAN−NH_2 of the lowest RGC (type a, 0.004 mol NH_2/wt %) and all the SAN−carb samples align on the same curve. This dependence is initially linear, in agreement with the interfacial reaction rate equation proposed earlier (eq 1). Thus, the amount of SAN bound at the interface is controlled by the reduced [X]/[MA] molar ratio, and the interfacial grafting is 3.3 times more rapid in the case of primary amine.

Beyond a critical reduced molar ratio, i.e., ca. 3, the slope of this dependence becomes very small because of the occupancy of the interface by the already formed copolymer.[32,33] At a critical reduced molar ratio, and thus at a critical grafting yield, there is a change in the grafting regime form a grafting limited by the concentration of the reactive groups near or at the interface to a grafting limited by the steric protection of the interface by the graft copolymer itself. Note that the particle size levels off at a lower critical reduced [X]/[MA] molar ratio (i.e., ca. 2 in Figure 3) compared to the SAN grafting (ca. 5). As a rule, the interface does not need to be saturated by graft copolymer in order to prevent the coalescence of the dispersed rubber droplets from occurring, in contrast to the impact strength that needs more extensive interfacial modification.

The RGC of reactive SAN however affects the SAN grafting in a way that depends on the reactive groups. Indeed, in the case of SAN−NH_2, the amount of grafted SAN decreases as the RGC is increased, at constant [NH_2]/[MA] ratio, although it is independent of the RGC of SAN−carb. This difference in behavior of SAN−NH_2

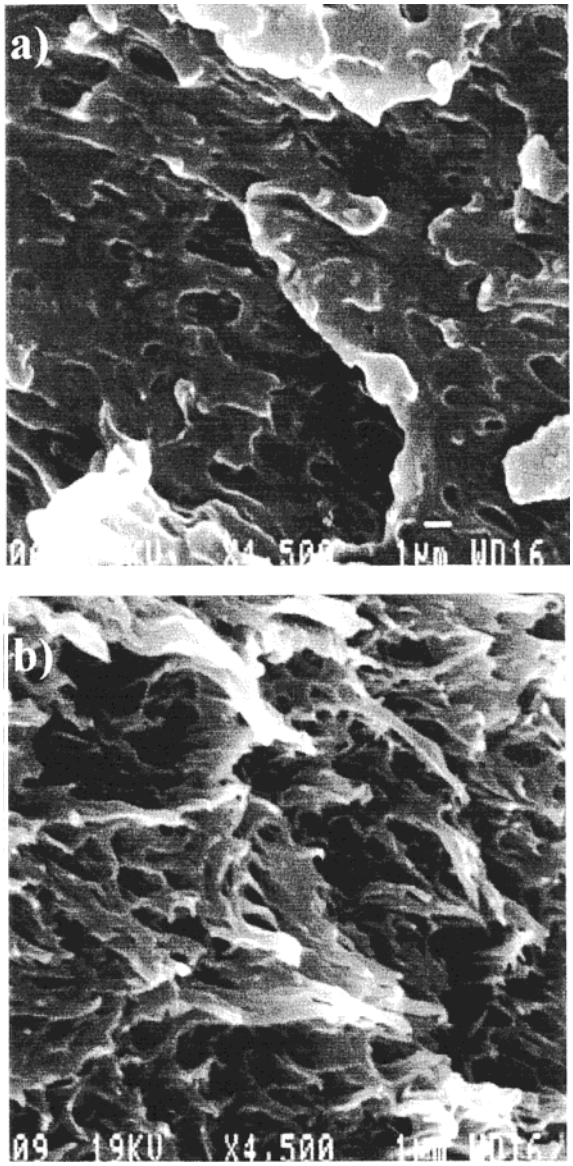

Figure 9. SEM of the impact fracture surface of the (SAN/SAN−NH_2 8/2)/(EPDM/EP-*g*-MA 1/1) 75/25 reactive blend (SAN−NH_2 type B, 0.028 mol NH_2/wt %) (a) near the notch and (b) far from the notch.

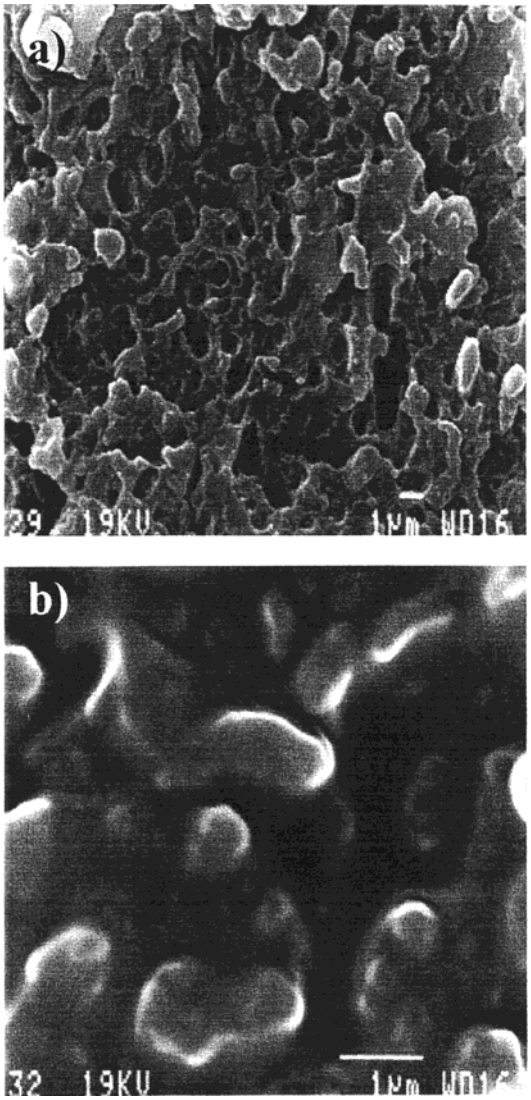

Figure 10. (a) SEM of the impact fracture surface (observation far from the notch) of the (SAN/SAN−NH_2 8/2)/(EPDM/EP-*g*-MA 1/1) 75/25 reactive blend (SAN−NH_2 type C, 0.049 mol NH_2/wt %) and (b) at higher magnification.

and SAN−carb can be explained by the grafting kinetics.

Indeed, in the case of SAN−carb, the interfacial grafting is controlled by the carbamate thermolysis into primary amine,[13,14] at a rate constant of 0.0084 min^{-1}. The reactive amine groups are thus regularly released all along the mixing process. For instance, the amine released after 7 min mixing (which is the residence time in the mixer) amounts to ca. 6% of the original carbamate content, i.e., 0.23 (type a), 1.6 (type b), and 2.8 (type c) amines per reactive SAN chain ($M_n = 10^5$ g/mol). At constant [carb]/[MA] molar ratio, the amount of SAN−carb in the SAN phase decreases when the RGC is increased. However, in parallel, the probability that each chain SAN−carb chain reacts at the interface increases with the RGC. So, the final SAN−carb conversion is essentially independent of the RGC, as experimentally observed in the limits of this investigation (Figure 11). Furthermore, the small number of amines released per SAN−carb chain (0.23−2.8) suggests that when one SAN−carb chain is grafted to the interface, the chance for second carbamate group of the same chain to be transformed into amine and to react at the interface is low enough for another chain to compete

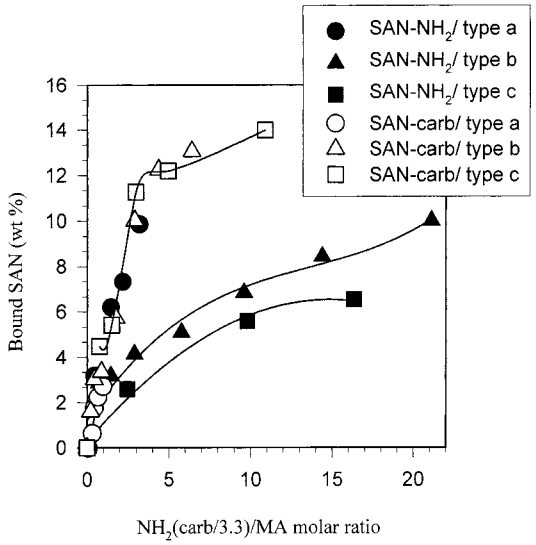

Figure 11. Dependence of the amount of bound SAN on the reduced carb(NH_2)/MA molar ratio for the SAN/EPR 75/25 polyblend modified by SAN−carb(NH_2) of various reactive groups contents (type a, 0.004; type b, 0.028; type c, 0.049; type d, 0.078 mol/wt % of either NH_2 or carbamate) in the SAN phase and 50 wt % EP-*g*-MA in the EPR phase.

efficiently for grafting at the same interface.

In the case of SAN−NH_2, the X−MA interfacial reaction is much faster, all the X functional groups (in the range of 4−49 amines per chain) being intrinsically reactive toward MA in contrast to the carbamate ones. As speculated elsewhere,[14] when an amine group of a highly functional SAN−NH_2 chain reacts at the surface of a rubber particle, the other amine groups of this anchored chain have a much higher probability of reacting at the same interface compared to amine groups of still unanchored SAN chains localized farther from the interface.[3,4] The SAN−NH_2 chains are then expected to react through multiple bonding in a strong dependence on the RGC of reactive SAN. As a result, when the RGC of SAN−NH_2 is increased at constant [NH_2]/[MA] molar ratio, the amount of SAN−NH_2 in the SAN phase decreases, and fewer SAN chains are grafted at the interface, as confirmed by Figure 11. Figure 12 is a tentative sketch of the architecture of the graft copolymer which is formed in relation to the way the interfacial grafting reaction occurs.

3.6. Interfacial Conformation of the Bound SAN Chain. The knowledge of the particle size (Figure 3, eqs 5 and 6) and the amount of grafted SAN (Figure 11) allows the interface area occupied per grafted SAN chain (A) to be calculated, assuming that the SAN-*g*-EP copolymer formed by reactive processing remains at the interface and that the SAN average molecular weight (M) is 10^5 g/mol[13,14] (eq 7):

$$A = 6M\phi_d/(N_{av}D_nW) \qquad (7)$$

where N_{av} is the Avogadro number, W is the mass of bound SAN per unit volume of blend, D_n is the number-average diameter, and ϕ_d is the volume fraction of the dispersed phase. The results are reported in Table 3 for polyblends modified by reactive SAN of type a, b, and c in relation to the reduced [X]/[MA] molar ratio. As a rule, the area stabilized per bound SAN chain, A, decreases regularly when the reduced [X]/[MA] molar ratio is increased. Furthermore, at constant [NH_2]/[MA] ratio, the cross-sectional surface area per bound SAN−

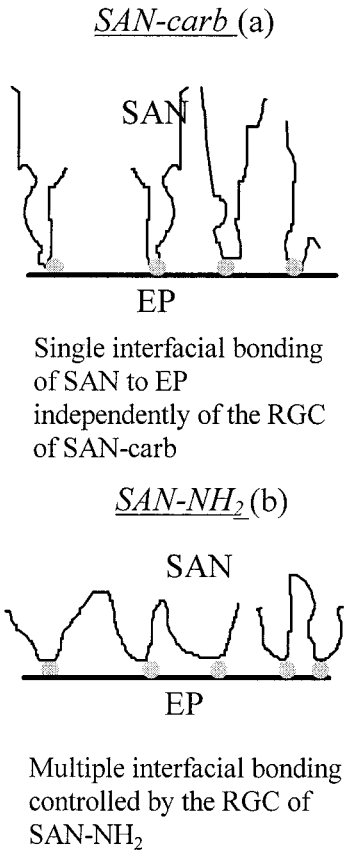

Figure 12. Tentative schematic view of the architecture of the graft SAN chain.

Table 3. Calculated Cross-Sectional Surface Area per Bound SAN Chain (*A*) and Experimental Impact Strength vs Reduced NH_2(carb)/MA Molar Ratio[a]

		cross-sectional surface area per bound SAN chain (nm^2)[c]		
NH_2(carb/3.3)/MA	D_n[b] (μm)	all SAN−carb + type a/NH_2	type b/NH_2	type c/NH_2
1	0.88	14.5 (15)[d]	23.2 (12)	43.3 (8)
2	0.48	11.3 (25)	26.4 (19)	39.6 (13)
3	0.42	9.05 (30)	22.6 (25)	30.2 (17)
5	0.41	7.75 (38)	17.4 (32)	25.10 (21)
10	0.41	6.64 (43)	13.3 (35)	16.7 (23)

[a] The EPR phase contains 50 wt % EP-*g*-MA and the SAN phase different amounts of SAN−X of various reactive groups contents: 0.004 (type a), 0.028 (type b), 0.049 (type c), and 0.078 (type d) mol X/wt % (X being NH_2 or carbamate). [b] Extracted from eqs 5 and 6. [c] Based on eq 7. [d] Charpy impact strength in parentheses.

NH_2 chain increases with the RGC, in contrast to the independence observed for the SAN−carb chains. Therefore, the extent of SAN functionalization (RGC) affects in different ways the conformation of the SAN chain grafted at the interface depending on the course of the grafting reaction (i.e., primary amine vs carbamate). These data confirm that the grafted SAN−NH_2 chains are more extensively spread over the interface through multiple interfacial bonding in a strong dependence on the RGC, compared to SAN−carb chains, that would be rather tethered to the interface, in agreement with Figure 12. Therefore, in the case of SAN−NH_2 of high RGC, a lower amount of bound SAN chains is required to stabilize comparable particle size than in the case of SAN−carb or SAN−NH_2 of low RGC, as inferred from the comparison of Figures 3 and 11.

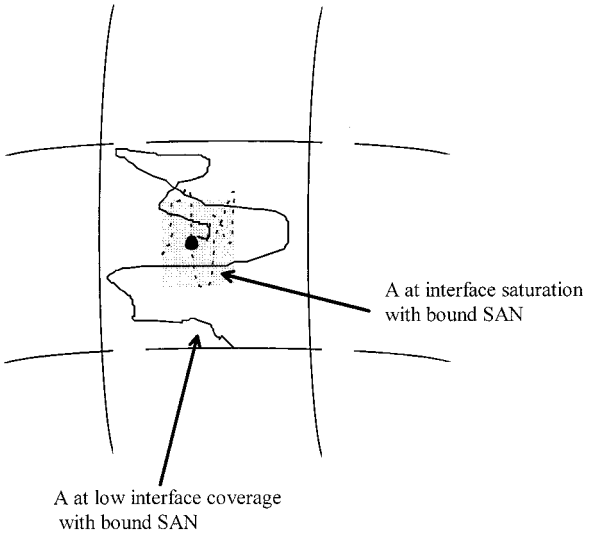

Figure 13. Tentative schematic view of the cross-sectional surface area per bound SAN (*A*) (single bonding, Figure 12a) vs the interface coverage with graft SAN.

It is noteworthy that the particle size beyond a critical reduced [X]/[MA] molar ratio of ca. 2 levels off (Figure 3), in contrast to the SAN grafting (Figure 11) and the area stabilized per SAN chain (Table 3) that goes on changing. Beyond this critical molar ratio of 2, the total interfacial surface area remains constant, and more chains are grafted, leading to grafted chains of more packed conformation and thus stabilizing a smaller surface area *A* (Figure 13).

The loss in ductility which is observed when the RGC of SAN−NH_2 is increased (Figure 4) can be accounted for by the multiple grafting of the SAN−NH_2 chains of high RGC that accordingly form loops of shorter length, thus less prone to be entangled with the ungrafted SAN chains and to anchor efficiently SAN to EPR.[3] Convincingly, the fracture mechanism has been found to change from rubber fibril fracture to detachment of bound SAN chains from the SAN matrix, as the SAN amine content was exceeding 0.028 mol/wt %, in line with the fracture surface reported in Figure 10.

Figure 14 that shows the dependence of both the impact strength and the number-average diameter of rubber particles on the reduced [X]/[MA] molar ratio, together with the interfacial area stabilized per bound SAN, summarizes the situation. The reduced [X]/[MA] molar ratio expresses the extent of the interfacial reaction which controls the rubber dispersion independent of the content and type of SAN reactive groups. The decrease of D_n upon increasing reduced [X]/[MA] ratio is the signature of the increasing formation of interfacial chain entanglements. It must be kept in mind that the carbamate content is divided by 3.3 in the reduced molar ratio, indicating that 3.3 more carbamate groups are required to provide the same particle size as in the case of primary amine. Thus, use of SAN−NH_2 is comparatively more economic than SAN−carb.

Nevertheless, although the interfacial adhesion must increase with the number of bridges at the interface, the effectiveness of the entanglements of the bound SAN−NH_2 with the SAN matrix decreases with increasing RGC. Indeed, SAN−NH_2 chains of high RGC are extensively spread over the interface (high value of *A*) through multiple bonding, giving more loops per bound chain, but with lower probability of entanglement with the matrix. This explains that, at constant rubber

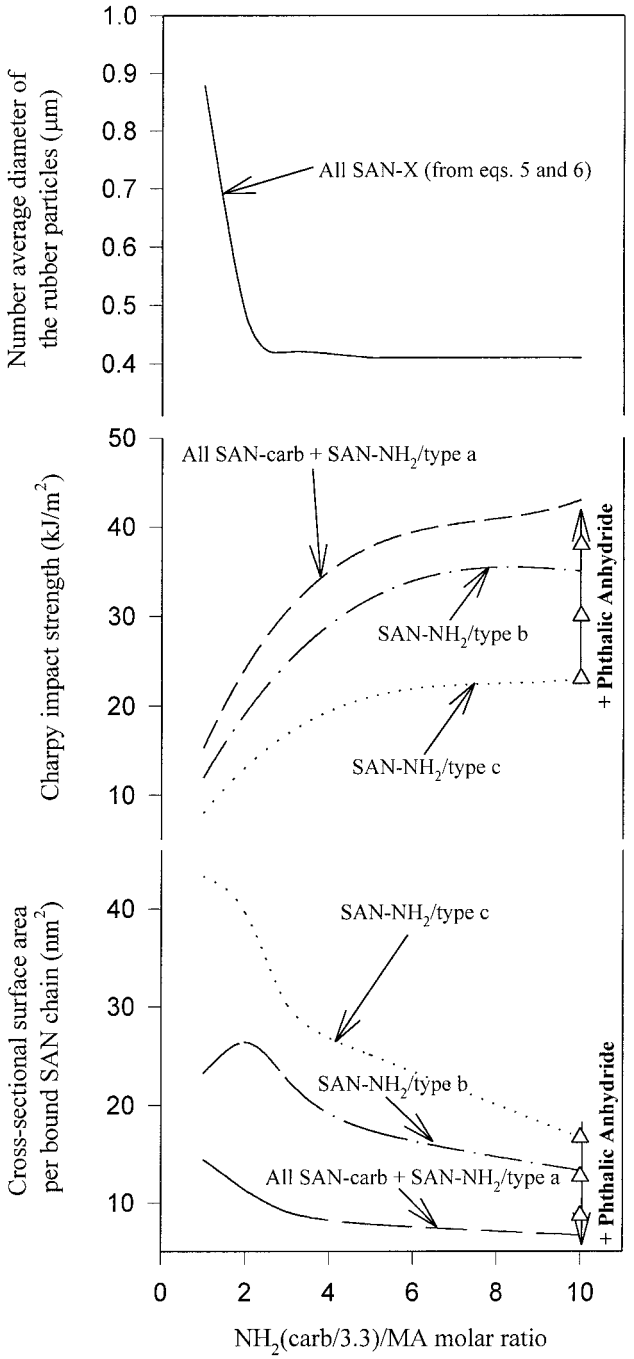

Figure 14. Dependence of the number-average rubber particle diameter (from eqs 5 and 6, Figure 3), the notched Charpy impact strength (from Figure 5), and the cross-sectional surface area per bound SAN chain (A from Table 4) on the reduced carb(NH_2)/MA molar ratio for the 75/25 SAN/EPR polyblend modified by SAN−carb(NH_2) of various reactive groups contents (type a, 0.004; type b, 0.028; type c, 0.049; type d, 0.078 mol/wt % of either NH_2 or carbamate) in the SAN phase and 50 wt % EP-*g*-MA in the EPR phase.

particle size, the RGC of of SAN−NH_2 has a deleterious effect on the impact strength. Thus, at constant particle size, SAN−carb imparts better interfacial adhesion[34] and toughness to the blends than SAN−NH_2, since the bound SAN−carb chains are essentially tethered at the interface (low value of *A*), and more prone to be entangled with the ungrafted chains and to anchor efficiently SAN to EPR, independent of the RGC.

3.7. Progress in Toughening SAN. If the aforementioned hypothesis on the interfacial conformation of the bound SAN chain is correct, then the very fast deactivation of the amine groups still available on the grafted SAN chains should decrease both the average number of grafting sites per chain and the area occupied per SAN−NH_2 chain grafted at the interface. This strategy should lead to SAN−NH_2 chains more tethered at the interface, all the other conditions being the same. For this purpose, phthalic anhydride has been added to the reactive blends containing 20 wt % SAN−NH_2 (type c) in the SAN phase. This strategy has been proposed by Maréchal et al. in the case of the reactive blending of EP-*g*-MA and Nylon 6.[35,36] Under the usual processing conditions, the toughness of the final polyblend is poor (ca. 20 kJ/m^2). Phthalic anhydride, which is expected to compete with EP-*g*-MA for reaction with SAN−NH_2, has been premixed with the rubber phase in order to favor its reaction with SAN−NH_2 present at the interface. The impact properties of the reactive blends modified by increasing amounts of phthalic anhydride are reported in Table 4, together with the values of *A*, as calculated by eq 7. Phthalic anhydride clearly improves the toughness of the SAN/rubber polyblend. The Charpy impact strength continuously increases with the phthalic anhydride content (at least within the studied concentration range). Compared to brittleness in the absence of phthalic anhydride (20 kJ/m^2), blends containing 2 wt % phthalic anhydride show a ductile behavior (38 kJ/m^2), and the fracture mechanism operating based on rubber fibril fracture is restored. It thus appears that phthalic anhydride reacts faster at the interface with SAN−NH_2 than EP-*g*-MA (at 200 °C, the anhydride is a liquid). The parallelism between the increase in the impact strength and the decrease of *A* with the phthalic anhydride/NH_2 molar ratio is shown in Figure 15 and gives credit to more efficient chain entanglements when the grafted chains are tethered. As expected, upon addition of increasing amount of phthalic anhydride, the high RGC SAN−NH_2 (type c) changes progressively of interfacial conformation at the interface and attains the mechanical performance of SAN−carb or low RGC SAN−NH_2, at constant particle size (Figure 14).

Table 4. Calculated Cross-Sectional Surface Area per Bound SAN Chain (*A*), Elongation at Break (ϵ_b), Notched Charpy Impact Strength for 75/25 SAN/EPR Polyblend Containing 20 wt % SAN−NH_2 in the SAN Phase (Type c, 0.049 mol NH_2/wt %) and 50 wt % EP-*g*-MA Plus Increasing Amounts of Phthalic Anhydride in the EPR Phase

phthalic anh (wt %)[a]	anh/NH_2 molar ratio[b]	ϵ_b (%)	impact (kJ/m^2)	*A* (nm^2)[b]
0	0	11	22 ± 0.5	16.7
0.5	0.46	15 ± 5	25 ± 5	15.8
1	0.92	14.5 ± 0.2	27 ± 1	15.7
1.5	1.38	23 ± 2	30 ± 1	12.7
2	1.84	30 ± 1	38 ± 2	8.7

[a] With respect to the whole blend. [b] Based on eq 7.

4. Conclusions

In this study, special attention has been paid to the influence of the kinetics of the interfacial reaction on the SAN/EPR compatibilization. For this purpose, the three main reaction parameters have been varied, i.e., the intrinsic reactivity of the functional groups attached onto SAN (k_{NH_2} vs k_{carb}), the content of these reactive groups (RGC, between 0.004 and 0.078 mol X/wt %), and the amount of reactive SAN in the 75/25 wt/wt SAN/EPR blend (in the range of 2.5 and 73.33 wt %).

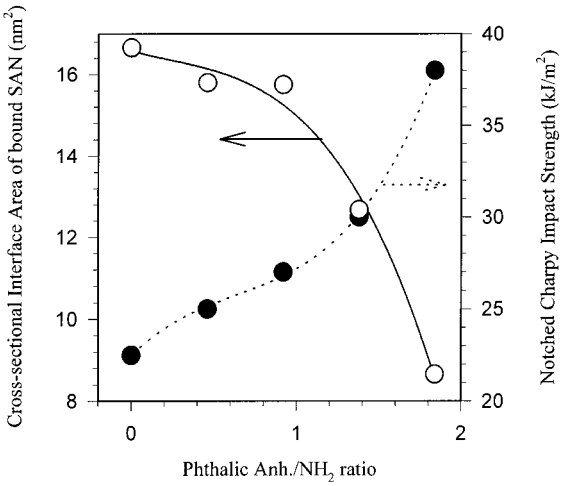

Figure 15. Dependence of both the notched Charpy impact strength and the cross-sectional surface area per bound SAN chain (A from Table 4) on the phthalic anhydride/amine molar ratio for the SAN/EPR 75/25 polyblends modified by 20 wt % SAN−NH_2 (type c, 0.049 mol NH_2/wt %) in the SAN phase and 50 wt % EP-*g*-MA plus increasing amounts of phthalic anhydride in the EPR phase.

The polyblends properties have been discussed on the basis on both the number and the effectiveness of interfacial entanglements in situ formed, in relation to the molecular structure of SAN−X.

The effect of the intrinsic reactivity of the SAN reactive groups, i.e., NH_2 vs carbamate, has been clearly demonstrated by the differences observed in the emulsification efficiency. In agreement with the comparatively higher reactivity of the primary amine compared to the carbamate toward maleic anhydride, less NH_2 groups are required to achieve comparable particle size. Since less material is needed, SAN−NH_2 is more viable from an economic point of view than the SAN−carbamate counterpart.

At constant particle size, the RGC of the reactive SAN chains affects in different ways the impact properties, in a way that depends on the reactive groups (primary amine or carbamate). In the case of SAN−NH_2, increasing RGC has a deleterious effect on the impact resistance, as result of more grafting sites per SAN chain, so that the length of the loops formed on the rubber particle surface decreases and the probability of entanglement with the matrix, as well. In contrast, in the case of SAN−carb, the RGC has no marked effect on the conformation of the grafted chains, which are basically tethered at the interface and prone to be entangled with the SAN chains in the matrix. Thus, when the final phase morphology is reached, SAN−carb promotes higher impact strengths than SAN−NH_2, even though more carbamate groups are needed due to a lower reactivity.

It can be concluded that the number and type of reactive groups attached onto SAN affect not only the extent of the compatibilization reaction but also the compatibilization capability of the graft copolymer in situ formed in a strong dependence on molecular weight and molecular architecture.

Acknowledgment. C.P. and R.J. are grateful to the "Services Fédéraux des Affaires Scientifiques, Techniques et Culturelles" for general support in the frame of the "PAI-4: Chimie et Catalyze Supramoléculaire". They also thank Dr. I. Luzinov for stimulating and helpful discussions and Mrs. M. Dejeneffe for assistance with cryoultramicrotomy. The authors are much indebted to DSM for financial support and a fellowship to one of them (C.P.).

References and Notes

(1) De Roover, B. Ph.D. Thesis, Université Catholique de Louvain, 1994.
(2) Lavengood, R. E. Eur. Patent, No. 202214, Monsanto Company, 1986.
(3) Chen, L.; Wong, B.; Baker, W. E. *Polym. Eng. Sci.* **1996**, *36*, 1594.
(4) Duvall, J.; Selliti, C.; Myers, C.; Hiltner, A.; Baer, E. *J. Appl. Polym. Sci.* **1994**, *52*, 195.
(5) Van Duin, M.; Koning, C. E.; Pagnoulle, C.; Jérôme, R. *Prog. Polym. Sci.* **1998**, *23*, 707.
(6) Hu, G. H.; Lambla, M. *J. Polym. Sci., Part A* **1995**, *33*, 97.
(7) Pagnoulle, C.; Koning, C. E.; Leemans, L.; Jérôme, R. Dutch Application No. 1007074, 1997.
(8) England, W. P.; Stoddard, G. J.; Scobbo, J. J. US Patent No. 5310795, 1994.
(9) Pagnoulle, C.; Jérôme, R. Polyblends'97, SPE Retec, Oct 9−10, 1997, IMI Boucherville, QC, Canada, oral communication. Pagnoulle, C.; Koning, C. E.; Leemans, L.; Jérôme, R. *ACS PMSE Prepr.* **1998**, *79*, 104.
(10) Scott, C. E.; Macosko, C. W. *Polym. Bull.* **1991**, *26*, 341.
(11) Favis, B. D. *J. Appl. Polym. Sci.* **1990**, *39*, 285.
(12) Plochocki, A. P.; Dagli, S. S.; Andrews, R. D. *Polym. Eng. Sci.* **1990**, *30* (12), 741.
(13) Pagnoulle, C.; Koning, C.; Van Duin, M.; Jérôme, R. *Macromolecules* **2000**, *33*, 6275.
(14) Pagnoulle, C. Ph.D. Thesis, University of Liège, Feb 1999.
(15) Cigana, P.; Favis, B. D.; Jérome, R. *J. Polym. Sci.* **1996**, *34*, 1691.
(16) Tang, T.; Hang, B. *Polymer* **1994**, *35*, 281.
(17) Bragaw, C. G. *Adv. Chem. Ser.* **1971**, *99*, 86.
(18) Kambour, R. P. *J. Polym. Sci., Part A-2* **1966**, *4*, 17.
(19) Wu, S. *Polym. Eng. Sci.* **1990**, *30* (13), 753.
(20) Hu, G. H. *J. Polym. Sci., Part B* **1998**, *36*, 2153.
(21) Sundararaj, U. Ph.D. Thesis, University of Minnesota, Jan 1994.
(22) Khandpur, A. K.; Nakayama, A.; Marechal, P.; Inoue, T. *Macromolecules* **1996**, *29*, 5590.
(23) Liu, N. C.; Baker, W. E. *Polym. Eng. Sci.* **1988**, *28*, 1427.
(24) Bucknall, C. B. *Toughened Plastics*; Applied Science Publishers: London, 1977.
(25) Durst, R. R.; Griffith, R. M.; Urbanic, A. J.; van Essen, W. J. *Am. Chem. Soc. Prepr., Org. Coat. Plast. Chem.* **1974**, *34*, 320.
(26) Newman, S. *Polym. Plast. Technol. Eng.* **1974**, *2*, 67.
(27) Duvall, J.; Sellitti, C.; Myers, C.; Hiltner, A.; Baer, E. *J. Appl. Polym. Sci.* **1994**, *52*, 207.
(28) Shull, K. R. *Macromolecules* **1992**, *25*, 2637.
(29) Brown, H. R. *J. Mater. Sci.* **1990**, *25*, 2791.
(30) Cho, K.; Brown, H. R.; Miller, D. C. *J. Polym. Sci., Polym. Phys. Ed.* **1990**, *28*, 1699.
(31) Matsuhita, Y.; Mori, K.; Saguchi, R.; Norda, I.; Nagosawa, M.; Chang, T.; Glinka, C. J.; Han, C. C. *Macromolecules* **1990**, *23*, 4387.
(32) Orr, C. A.; Adedeji, A.; Hirao, A.; Bates, F. S.; Macosko, C. W. *Macromolecules* **1997**, *30*, 1243.
(33) Hugenard, C.; Varoqui, R.; Pefferkorn, E. *Macromolecules* **1991**, *24*, 2226.
(34) Pagnoulle, C.; Jérôme, R. *Macromol. Symp.* **2000**, *149*, 207.
(35) Maréchal, Ph. Ph.D. Thesis, Catholic University of Louvain, Louvain-la-Neuve Belgium, June 1993.
(36) Maréchal, Ph.; Dekoninck, J. M.; Legras, R. Fourth European Symposium on Polymer Blends; Capri, Italy, May 23−26, 1993.

MA000822G